JCAMECH

Vol. 50, No. 1, June 2019, pp 1-13
DOI:10.22059/jcamech.2017.239277.173

Elasto-plastic solution for thick-walled spherical vessels with an inner FGM layer

Amin Seyyed Nosrati[a], Ali Parvizi[a,], Seyyed Ali Afzal[a], Vali Alimirzaloo[b]*

[a] *School of Mechanical Engineering, College of Engineering, University of Tehran, Tehran, Iran*
[b] *Engineering Department, Urmia University, Urmia, Iran*

ARTICLE INFO

Article history:
Received
Received in revised form
Accepted
Available online

Keywords:
Thick-walled sphere,
Elasto-plastic analysis,
FG Coating,
Pressure.

ABSTRACT

Purely elastic, partially and fully plastic stress states in a thick-walled spherical pressure vessel with an inner functionally graded material (FG) coating subjected to internal and external pressures are developed analytically in this paper. The modulus of elasticity and the uniaxial yield limit of the FG coating layer are considered to vary nonlinearly through the thickness. Using Tresca's yield criterion and ideal plastic material behavior, the plastic model is established. Under pressure loading, the scenario in which the plastic deformation starts from inner surface of FG coating layer is taken into account. Having increased the pressure loading, it is assumed that the FG coating layer becomes fully plastic and the yielding commences subsequently at the inner surface of homogenous part. Essentially, the variation of FG parameters in the radial direction is properly adjusted in order to achieve the stated yielding scenario. Furthermore, axisymmetric finite element model is performed to validate the accuracy of the analytical results. It is concluded that the elastic and plastic response of the spherical pressure vessel are influenced by grading parameters and coating behavior.

1. Introduction

Functionally graded materials (FGMs) are the nonhomogeneous composite materials in which mechanical properties vary continuously from one surface to the other by varying the volume fraction of their constituent, gradually. The FGMs have aerospace applications such as thermal barrier materials [1, 2].

A thick-walled pressure vessel under internal and external pressure is one of the prevalent problems in engineering mechanics. Pressure vessels have enormous industrial applications, such as the nuclear, oil, petrochemical, and chemical fields [3]. The FGMs are used in pressure vessels containing high temperature fluids in different industries because of their advantage of both mechanical and thermal properties, simultaneously. FG coatings can be used in pressure vessels due to their protective role for metallic or ceramic substrates against heat penetration, wear, corrosion and oxidation [4].

Having investigated the literature of functionally graded (FG) spheres and cylinders, it is known that there are several investigations dealing with the stress analysis of spherical and cylindrical pressure vessels subjected to pressure loading. Bufler [5] developed the analysis of laminated composite hollow spheres under internal and/or external pressure. Eslami et al. [6] carried out an analytical study to obtain the thermal and mechanical stresses in a hollow thick sphere made of functionally graded material. Considering heat conduction and Navier equations, they also obtained the radial stress, hoop stress, radial displacement and temperature profile as a function of radial coordinate. You et al. [7] studied the elastic response of hollow spheres made of functionally graded materials subjected to internal and external pressure. Two different kinds of pressure vessels were considered in their study: FG vessel and a vessel consists of two homogeneous layers with FG layer in between. Poultangari et al. [8] performed an analytical study to obtain the thermal and mechanical stresses in a FG sphere vessel under non-axisymmetric thermomechanical loads. Chen and Lin [9] carried out an analysis to obtain the elastic response of thick FG spherical vessels considering exponential variation of Young's modulus.

Presenting a new approach, Tutuncu and Temel [10] performed an analytical study to obtain stress components in the

[*] Corresponding author. E-mail address: aliparvizi@ut.ac.ir, Tel: +98 21 61119953

pressurized hollow FG cylinders, disks, and spheres. Taking into account linear and exponential material variation patterns, Saidi et al. [11] presented an exact closed-form solutions to obtain displacement and stresses in the thick-walled FG spherical pressure vessels. Sadeghian and Toussi [12] obtained elastic and perfectly plastic thermal stresses in a FG spherical vessel subjected to thermal and mechanical loading. In their study, both mechanical and thermal properties were assumed to vary in the radial direction according to power law function. Using a layerwise mixed shell theory, Carrera and Soave [13] analyzed the stresses in a composite pressure vessel with an interlayer of FG subjected to mechanical and thermal loadings. Parvizi et al. [14] presented an analytical elastic-plastic solution for thick-walled cylinders made of FG AlA359/SiCp subjected to internal pressure and thermal loading.

Based on power-law variation of material properties, analytical and numerical studies for a FG hollow sphere subjected to mechanical and thermal loads were presented by Bayat et al. [15]. Moreover, they carried out finite element simulation of process to verify the accuracy of the analytical solution. Nejad et al. [16] presented an exact closed-form solutions for stresses and displacements in FG thick-walled pressurized spherical shells. They assumed an exponential law formula for variation of material properties. Boroujerdy and Eslami [17] evaluated thermal instability of shallow spherical shells made of FG and surface-bonded piezoelectric actuators. They obtained the equilibrium equations based on the classical theory of shells and the Sanders nonlinear kinematics equations. Saadatfar and Aghaie-Khafri [18] investigated static behavior of a FG magneto-electro-elastic hollow sphere under hydrothermal loading in the spherically symmetric state. They assumed Winkler elastic foundation on the inner and/or outer surfaces of the sphere and a power law variation in material properties. Considering the combined uniform pressure and thermal loading condition, Parvizi et al. [19] presented an exact analytical thermo-elasto-plastic solution for thick-walled spheres made of FGMs. Considering three different plasticization from inner, through thickness and outer radii, they formulated the problem and validated the results by FE model. Alikarami and Parvizi [20] presented an exact theoretical elasto-plastic solution to obtain stress components for thick-walled cylinder made of FGMs subjected to combined pressure and thermal loading.

Akis [21] carried out an analytical study to obtain the elastic, partially plastic and fully plastic stress components in the spherical vessels made of FG materials under pressure. Atashipour [22] presented an analytical solution to obtain stress components in a thick-walled spherical homogeneous pressure vessel with an inner coating of FG material subjected to internal and external hydrostatic pressure. Loghman and Parsa [23] presented an analytical solution to obtain magneto-thermo-elastic response of a thick-walled cylinder with FG coating layer. They achieved the minimum stress and displacement condition by controlling the FG coating parameters. Wang et al. [24] studied the thermomechanical behavior of pressure vessel FG coating layer. Assuming tubular vessel with two hemisphere caps, they presented a close-form elastic solution and applied FE analysis to verify the theoretical results. Afshin et al. [25] presented a transient thermo-elastic analysis of a rotating thick cylindrical pressure vessel made of FGM subjected to axisymmetric mechanical and transient thermal loads under arbitrary boundary and initial conditions. They achieved the exact solution of time dependent temperature distribution and transient hoop, radial and axial stress components under general thermal boundary conditions. Gharibi et al. [26] studied stresses and the displacements of rotating exponential FGM thick hollow cylindrical under pressure using fundamental equations of elasticity and FSM. They obtained that the inhomogeneity constant provides a major effect on the mechanical behaviors of the exponential FG thick cylindrical under pressure. Ghajar et al. [27] presented the analysis of transient thermoelastic response of a FG non-axisymmetric viscoelastic cylinder. From the results of their study, it was concluded that, appropriate material inhomogeneities can improve the magnitudes of stress components, especially shear stress.

Reviewing the literature, it is found that the focus of the researchers was placed into the elastic and elasto-plastic analyses of homogenous and FG vessels. However, the investigation regarding thick-walled vessels comprising both homogenous and FG layers have remained so limited. Most of the above investigations were focused on the thick-walled hollow spheres with entire wall in FG while only a FG coating can be suitable for practical applications due to its reasonable manufacturing cost and avoid encountering technological limitations. Therefore, the elasto-plastic analysis of such spherical pressure vessels is important.

In this study, the elasto-plastic analytical solution for thick-walled spherical homogeneous pressure vessel with an inner FG coating subjected to hydrostatic pressure is presented for the first time. Having developed formulae for stresses and deformation in the vessel, the condition for incipient yielding at the inner surface of FG coating is established. Then, the condition for development of plastic zone in the FG layer is investigated and the stress field in both elastic and plastic regions of FG layer as well as the elasto-plastic boundary radius are obtained. After having a fully plastic FG layer, the condition for incipient yielding at the inner surface of homogenous material is evaluated. The similar analysis for development of plastic zone in the homogenous part is also carried out. The FE simulation of process was performed using ABAQUS/Explicit in order to validate the results of theoretical analysis.

2. Problem formulation

Fig. 1 shows the schematic of an internally coated spherical pressure vessel subjected to internal (P_i) and external (P_o) pressure. Here, R_i, R_o and R_c are the inner, outer, and the interface radii, respectively.

It is well-known that the strength of materials during a process is defined using the modulus of elasticity E and the yield limit σ_0 as the material properties. As a result, in this paper, these two material properties are assumed to vary in the radial direction for FG coating layer ($R_i < r < R_c$) of pressure vessel according to the relations

$$E(r)=E_0(\frac{r}{R_c})^n \ , \ \sigma_0(r)=\sigma_c(\frac{r}{R_c})^m \tag{1}$$

where E_0 and σ_c are the reference values of E and σ_0 in that order, r the radial coordinate and n and m are the grading parameters [21].

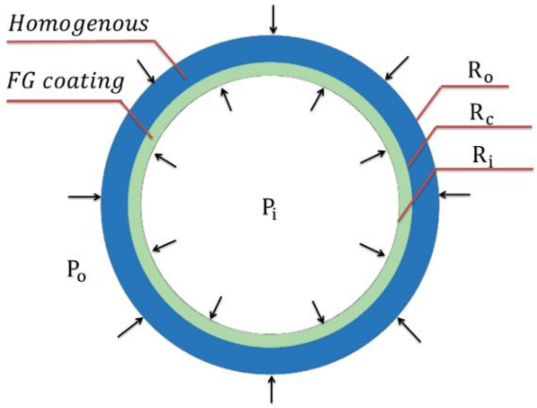

Fig. 1 An internally coated spherical pressure vessel under internal (P_i) and external (P_o) pressures

In this problem, spherical coordinates (r, θ, ϕ) are assumed. In addition, small deformations are considered in a loading spherical symmetry ($\sigma_\theta=\sigma_\phi$). Considering the conventional symbols for the stresses and strains [28], the Hooke's law reads

$$\varepsilon_r^T=\frac{1}{E(r)}[\sigma_r-2\upsilon\sigma_\theta]+\varepsilon_r^P \tag{2}$$

$$\varepsilon_\theta^T(=\varepsilon_\phi^T)=\frac{1}{E(r)}[(1-\upsilon)\sigma_\theta-\upsilon\sigma_r]+\varepsilon_\theta^P \tag{3}$$

where ε_i^P is the plastic strain components, ε_i^T is the total strain components, σ_i are the stress components in radial and circumferential directions, $E(r)$ the radius-dependent modulus of elasticity and ν the Poisson's ratio. Poisson's ratio is considered constant in vessel. It should be noted that values for Poisson's ratios in the coating layer and the wall of the vessel are assumed equal.

For elastic stress condition $\varepsilon_i^P=0$. Hence, using Eqs. (2) and (3) and strain-displacement relations ($\varepsilon_r^T=du/dr$ and $\varepsilon_\theta^T=u/r$), the stresses are written as

$$\sigma_r=\frac{E(r)}{(1+\upsilon)(1-2\upsilon)}[2\upsilon\frac{u}{r}+(1-\upsilon)\frac{du}{dr}], \tag{4}$$

$$\sigma_\theta(=\sigma_\phi)=\frac{E(r)}{(1+\upsilon)(1-2\upsilon)}[2\upsilon\frac{u}{r}+\upsilon)\frac{du}{dr}]. \tag{5}$$

The mechanical behavior of the structure is determined by the equilibrium equation, as follows:

$$\frac{d\sigma_r}{dr}+\frac{2}{r}(\sigma_r-\sigma_\theta)=0\ . \tag{6}$$

2.1. *Elastic solution*

2.1.1. *FG coating layer*

Supposing the variation of modulus of elasticity for coating material is according to the Eq. (1), the governing differential equation is obtained as

$$\frac{d^2u}{dr^2}+(\frac{2+n}{r})\frac{du}{dr}-\frac{2[1-\upsilon(1+n)]}{r^2(1-\upsilon)}u=0. \tag{7}$$

The general solution of above equation is

$$u^{C-E}=C_{1F}r^{-(1+n+K)/2}+C_{2F}r^{-(1+n-K)/2}. \tag{8}$$

where C_{1F} and C_{2F} are the arbitrary integration constants and

$$K=\sqrt{9+n(10+n-\frac{8}{1-\upsilon})}. \tag{9}$$

The stresses in the FG coating layer reduce to:

$$\sigma_r^{C-E}=\frac{E_0}{2(1+\upsilon)(1-2\nu)R_c^n}\left\{\begin{matrix}[(5+K+n)\upsilon-1-K-n]C_{1F}r^{-(3+K-n)/2}\\+[K(1-\upsilon)-n-1+(5+n)\upsilon]C_{2F}r^{-(3-K-n)/2}\end{matrix}\right\}, \tag{10}$$

$$\sigma_\theta^{C-E}=\frac{E_0}{2(1+\upsilon)(1-2\nu)R_c^n}\left\{\begin{matrix}[2-(1+K+n)\upsilon]C_{1F}r^{-(3+K-n)/2}\\+[2-(1-K+n)\upsilon]C_{2F}r^{-(3-K-n)/2}\end{matrix}\right\} \tag{11}$$

Here, superscript $C-E$ denote FG coating layer in elastic state.

2.1.2. *Homogeneous material*

Since the modulus of elasticity for homogeneous material is constant, the governing differential equation will be written as

$$\frac{d^2u}{dr^2}+\frac{2}{r}\frac{du}{dr}-\frac{2}{r^2}u=0, \tag{12}$$

The general solution of above equation is:

$$u^{H-E}=C_{1H}r+\frac{C_{2H}}{r^2} \tag{13}$$

where C_{1H} and C_{2H} are the arbitrary integration constants. Here, superscript $H-E$ denote homogenous body in elastic state.

Substituting Eq. (12) within Eqs. (4) and (5), the stresses in the homogeneous body reduce to:

$$\sigma_r^{H-E}=\frac{2E_0}{(1+\upsilon)(1-2\upsilon)}[(\upsilon+1)C_{1H}+(4\upsilon-2)\frac{C_{2H}}{r^3}], \tag{14}$$

$$\sigma_\theta^{H-E}(=\sigma_\varphi^{H-E})=\frac{E_0}{(1+\upsilon)(1-2\upsilon)}[(\upsilon+1)C_{1H}+(1-2\upsilon)\frac{C_{2H}}{r^3}]. \tag{15}$$

Using boundary and continuity conditions, the arbitrary integration constants are obtained for system of structure/coating.

Considering $P_o = 0$ and applying the hydrostatic pressure on inner and outer surfaces as boundary conditions:

$$\sigma_r^{H-E}(R_o) = 0, \tag{16}$$

$$\sigma_r^{C-E}(R_i) = -P_i, \tag{17}$$

and continuity conditions in the interface of vessel and coating in $r = R_c$:

$$u^{H-E}(R_c) = u^{C-E}(R_c), \tag{18}$$

$$\sigma_r^{H-E}(R_c) = \sigma_r^{C-E}(R_c), \tag{19}$$

By solving the four algebraic equations simultaneously, values of arbitrary integration constants are obtained.

2.2. *Onset of yield*

Yielding commences at the inner surface for a homogenous spherical pressure vessel as known from the previous studies [29].The relation $\sigma_\theta > \sigma_r$ is established for FG spherical pressure vessels subjected to internal pressure throughout just like in homogeneous ones. However, yielding could start at different surfaces of FG depending on the values of functionally grading parameters n and m. It is known from the previous studies [21] that, the parameter n has a greater influence on the yielding behavior. For the values of $n \geq 0$, the yielding may start at the inner surface, at the outer surface or at both surfaces of FG coating layer simultaneously. Furthermore, for the values of $n < 0$, the coating layer may fail at the inner or outer surfaces or inside the vessel. In this study, it is assumed that the yielding starts from the inner surface of FG coating layer of spherical pressure vessel. As a result, the positive value of n is considered.

For the values of $n \geq 0$, the yielding starts at the inner surface of FG coating layer at $r = R_i$ according to Tresca's yield criterion i.e. $\sigma_\theta - \sigma_r = \sigma_0$. The other modes of yielding onset for the values of $n > 0$ are not considered. The elastic limit internal pressure (P_{e1}) to start yielding at the inner surface of FG coating layer is determined by evaluating the coating layer stresses at R_i and using Tresca's condition. $\bar{P}_{ej}$ is the non-dimensional elastic limit pressure defined by $\bar{P}_{ej} = P_{ej}/\sigma_0(R_i)$. Furthermore, the elastic limit internal pressure (P_{e2}) to start plastic deformation at the inner surface of homogenous structure is determined by evaluating the homogenous structure stresses at R_c and using Tresca's condition.

Considering Tresca's yield criterion i.e. $\sigma_\theta - \sigma_r$, slight variation in the FG parameters causes change location from $r = R_i$ to $r = R_c$. As a result, there are critical parameters that would be start yielding concurrently at both surfaces. The corresponding conditions can be defined as:

$$\sigma_\theta^{C-E}(R_i) - \sigma_r^{C-E}(R_i) = \sigma_0(R_i), \tag{20}$$

$$\sigma_\theta^{H-E}(R_c) - \sigma_r^{H-E}(R_c) = \sigma_c. \tag{21}$$

If one of the parameters n, m and P_i to be set, the other two parameters are determined by solving Eqs. (20) and (21). Considering the given value of parameter n, the values of parameter m and the limit $\bar{P} = \bar{P}_{e1} = \bar{P}_{e2}$ can be obtained from Eqs. (20) and (21) is that the condition for the assembly to yield simultaneously at both surfaces. For example, assigning $\upsilon = 0.3$, $R_o/R_i = 2$, $R_c/R_i = 1.2$, $n = 0.9$, one finds $m = -2.3993$ and $\bar{P}_{e1} = \bar{P}_{e2} = 0.6325$ by solving Eqs. (20) and (21).

n and m values satisfying Eqs. (20) and (21) are donated as n_{cr} and m_{cr} to make clear the start of yield. If $n = n_{cr}$ and $m = m_{cr}$, then plastic deformation commences at both the inner surface of FG coating layer and inner surface of homogenous structure concurrently. If $m > m_{cr}$, then the assembly yields at the inner surface of FG coating layer and at the outer surface of coating layer when $m < m_{cr}$. Here, the condition of $m > m_{cr}$ is considered.

For $n = 0$ (constant E), one obtains $m_{cr} = -3$ and $\bar{P}_{e1} = 0.5833$ by the solution of the Eqs. (20) and (21). It has been reported that if $n = 0$ and $m = m_{cr} = -3$ at the elastic limit pressure $\bar{P}_{e1}$ on the spherical pressure vessel made by FG, the result of expression $\sigma_\theta^{C-E} - \sigma_r^{C-E}$ is constant and equal to σ_0 throughout the coating layer [21].

2.3. *Elasto-Plastic solution*

2.3.1. *FG coating layer*

Considering $\sigma_\theta > \sigma_r$ throughout the assembly, Tresca's yield criterion will be

$$\sigma_\theta^{C-E} - \sigma_r^{C-E} = \sigma_0. \tag{22}$$

Using the equilibrium equation, Eq.(6) and $\sigma_\theta^{C-E} = \sigma_r^{C-E} + \sigma_0$ from Eq. (22), the stress expressions in the plastic region are determined as

$$\sigma_r^{C-P} = C_3F + \frac{2(r/R_c)^m \sigma_c}{m}, \tag{23}$$

$$\sigma_\theta^{C-P} = C_3F + \frac{(2+m)(r/R_c)^m \sigma_c}{m}, \tag{24}$$

where C_{3F} is an unknown coefficient. Here, superscript $C-P$ denote FG coating layer in plastic state. Using these stresses, the incompressibility $\varepsilon_r^P + 2\varepsilon_r^\theta = 0$ and the strain-displacement relations, the expression $\varepsilon_r^T + 2\varepsilon_r^T$ is determined and simplified as follows:

$$\frac{du}{dr} + \frac{2u}{r} = F_1 r^{m-n} + F_2 C_{3F} r^{-n}, \tag{25}$$

where

$$F_1 = \frac{2R_c^{\,n-m}(3+m)(1-2\upsilon)\sigma_c}{mE_0}, \tag{26}$$

$$F_2 = \frac{2R_c^{\,n}(1-2\upsilon)}{E_0}. \tag{27}$$

The general solution is

$$u^{C-P} = \frac{C_{4F}}{r^2} + \frac{F_1}{m-n+3} r^{m-n+1} + \frac{F_2 C_{3F}}{3-n} r^{1-n}. \tag{28}$$

2.3.2. *Homogenous material*

The stresses at a homogenous spherical pressure vessel given by Mendelson [29] are

$$\sigma_r^{H-P} = C_{3H} + 2\sigma_c ln(r), \tag{29}$$

$$\sigma_\theta^{H-P} = C_{3H} + (2ln(r)+1)\sigma_c, \tag{30}$$

Where C_{3H} is an unknown coefficient. Here, superscript $H-P$ denote homogenous body in plastic state. Using these stresses, the incompressibility $\varepsilon_r^{\,P} + 2\varepsilon_r^{\,\theta} = 0$ and the strain-displacement relations, the expression $\varepsilon_r^{\,T} + 2\varepsilon_r^{\,T}$ is determined and simplified as follows

$$\frac{du}{dr} + \frac{2u}{r} = \frac{1-2\upsilon}{E_0}[3C_{3H} + 2\sigma_c + 6\sigma_c \ln(r)]. \tag{31}$$

The general solution is

$$u^{H-P} = \frac{C_{4H}}{r^2} + \frac{r(1-2\nu)[C_{3H} + 2\sigma_c ln(r)]}{E_0}. \tag{32}$$

3. Finite Element Simulation

The finite element simulation is applied using ABAQUS software to verify the accuracy of the present analytical solution. Fig. 2 shows FE model of spherical pressure vessel with FG coating layer. The axisymmetric model of the vessel is considered in order to reduce the computational cost. FG coating layer is divided into 10 layers along the radial direction to simplify the model. According to Eq. (1), the material properties of each section are calculated for FG coating. Considering the mesh sensitivity analysis, the model consists of 1320 CAX4T-type elements and 1395 nodes.

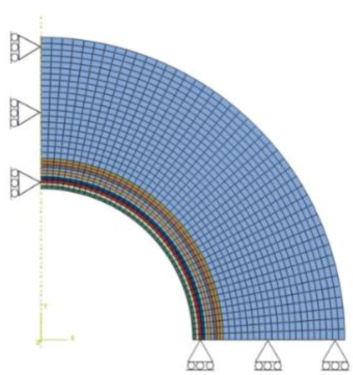

Fig. 2 FE model of spherical pressure vessel with inner FG coating divided into 10 sections

4. Results and discussion

The type of FG coating layer and the homogenous structure material used in the analysis is a steel ($E_0 = 200\ GPa$, $\nu = 0.3$, $\sigma_c = 430\ MPa$). Furthermore, the values of $R_o/R_i = 2$ and $R_c/R_i = 1.2$ are considered. The dimensionless variables are used to illustrate the numerical results as follows:

$$\bar{r} = \frac{r}{R_i}; \bar{\sigma} i = \frac{\sigma_i}{\sigma_0(R_i)}; \bar{u} = \frac{uE_0}{R_c \sigma_0(R_i)}. \tag{33}$$

4.1. *Elastic*

Considering $n = 0.9$, the elastic solution requires the determination of four unknown coefficients: C_{1H}, C_{2H}, C_{1F} and C_{2F}. The following four conditions are applied:

$$\sigma_r^{\,H-E}(R_o) = 0 \tag{34}$$

$$\sigma_r^{\,C-E}(R_i) = -P_i \tag{35}$$

$$u^{H-E}(R_c) = u^{C-E}(R_c) \tag{36}$$

$$\sigma_r^{H-E}(R_c) = \sigma_r^{C-E}(R_c) \tag{37}$$

Fig. 3 shows the variations of dimensionless radial stress, circumferential stress and displacement versus dimensionless radial coordinate ($\bar{r} = r/R_i$) at internally coated spherical pressure vessel. It is noteworthy that, the displacement and radial stress curve are continuous through the thickness, as expected. The trend of circumferential stress yields a slight change in the interface surface when shifting from FG coating layer to homogenous structure. Similar results have also reported by previous studies [22, 30]. It is obvious that there exists good agreement between analytical and FE results and the accuracy of analytical solution is verified. It should be noted that the good agreement between analytical and FE results can be seen in the following solutions of this study.

A dimensionless yield variable λ_y is presented to check the radial location of the yielding onset in elastic state [21]. Considering Tresca's yield criterion, the yielding starts at the radial location $r = r_y$ when

$$\sigma_\theta(r_y) - \sigma_r(r_y) = \sigma_0(r_y). \tag{38}$$

If the both sides divide by $\sigma_0(R_i) = \sigma_c(R_i/R_c)^m$, the simplified equation is

$$(\frac{R_i}{r_y})^m \times [\bar{\sigma}_\theta(r_y) - \bar{\sigma}_r(r_y)] = 1. \tag{39}$$

Therefore, the yield variable is defined as

$$\lambda_y = (\frac{R_i}{r_y})^m \times [\bar{\sigma}_\theta(r_y) - \bar{\sigma}_r(r_y)]. \tag{40}$$

It is notable that when $r = r_{ep}$, then $\lambda_y(r_{ep}) = 1$ at an elastic-plastic border, and $\lambda_y < 1$ in the elastic state.

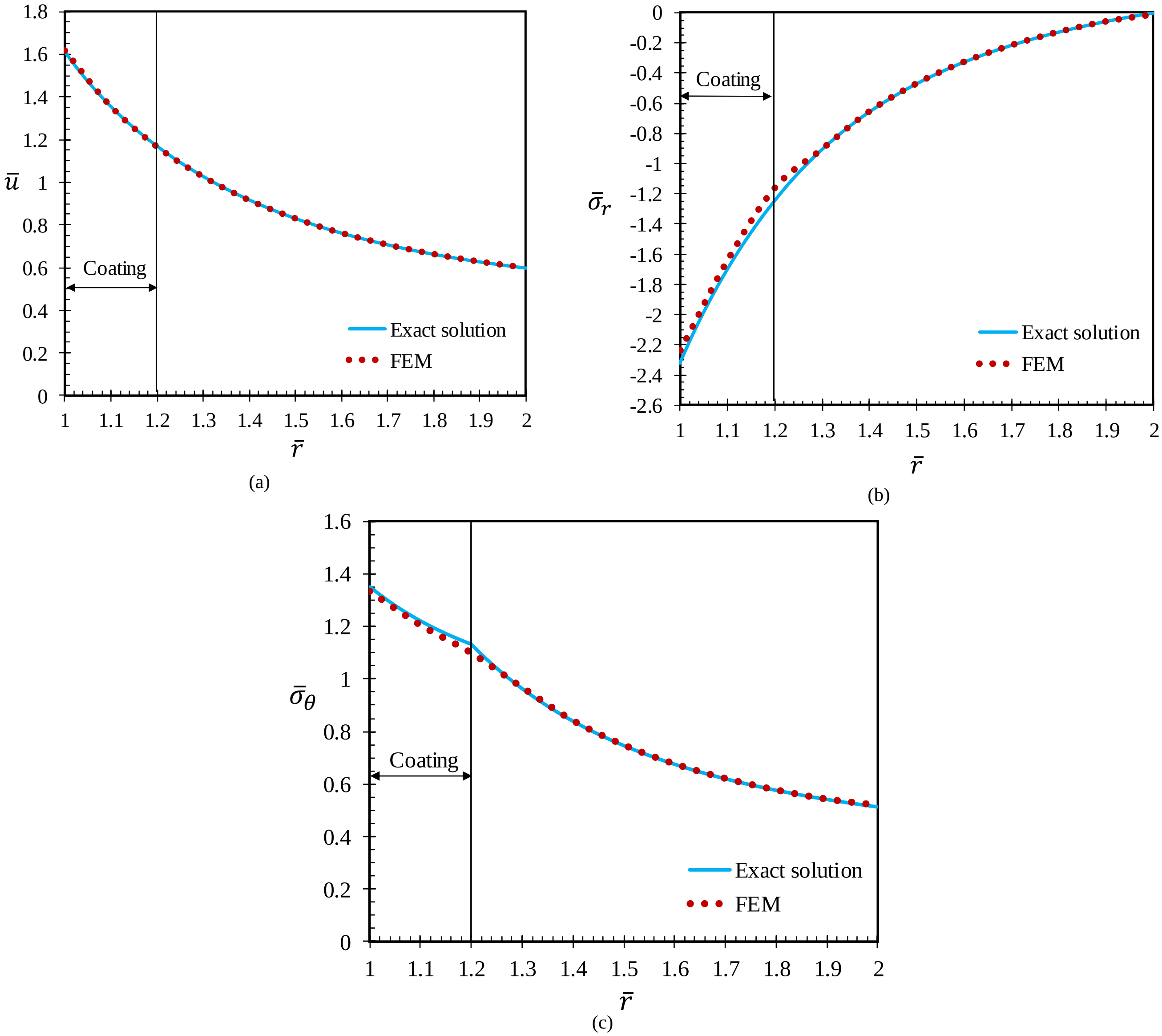

Fig. 3 Comparison of analytical results and FE solution for elastic response of internally coated spherical pressure vessel for $n = 0.9$ (a) displacement (b) radial stress (c) tangential stress

First, considering $n = 0.9$, the other critical FG parameter and the corresponding elastic limit internal pressure are calculated as $m_{cr} = -2.3993$ and $\bar{P}_{e1} = \bar{P}_{e2} = 0.6325$ by solving the Eqs. (20) and (21). Fig. 4 shows the corresponding yield variable at FG coating layer. As can be seen $\lambda_y = 1$ at the inner surface of FG coating layer and the inner surface of homogenous structure. It is clear that the yielding commences at the both surface simultaneously. However, it may not be easily distinguishable by following the stresses distribution near the both surface. The consequent stresses and displacement are shown in Fig. 5. From the data file of Fig. 5, it can be obtained that $\bar{\sigma}_r(1.2) = -0.3374$ and $\bar{\sigma}_\theta(1.2) = 0.3082$. Therefore, it follows that $\bar{\sigma}_\theta(1.2) - \bar{\sigma}_r(1.2) = 0.6456$, and further $\sigma_0(1.2) = (1.2)^m = (1.2)^{-2.3993} = 0.6456$, which validates $\bar{\sigma}_\theta(1.2) - \bar{\sigma}_r(1.2) = \bar{\sigma}_0(1.2)$.

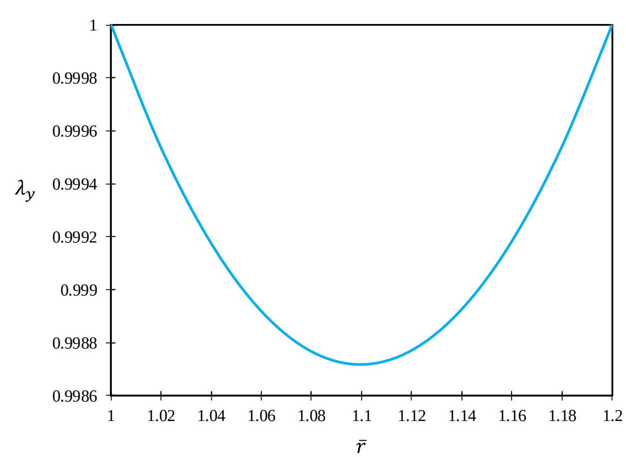

Fig. 4 Yield variable at FG coating layer of pressure vessel for $n = 0.9$, $m = m_{cr} = -2.3993$ at $\bar{P}_{e1} = \bar{P}_{e2} = 0.6325$

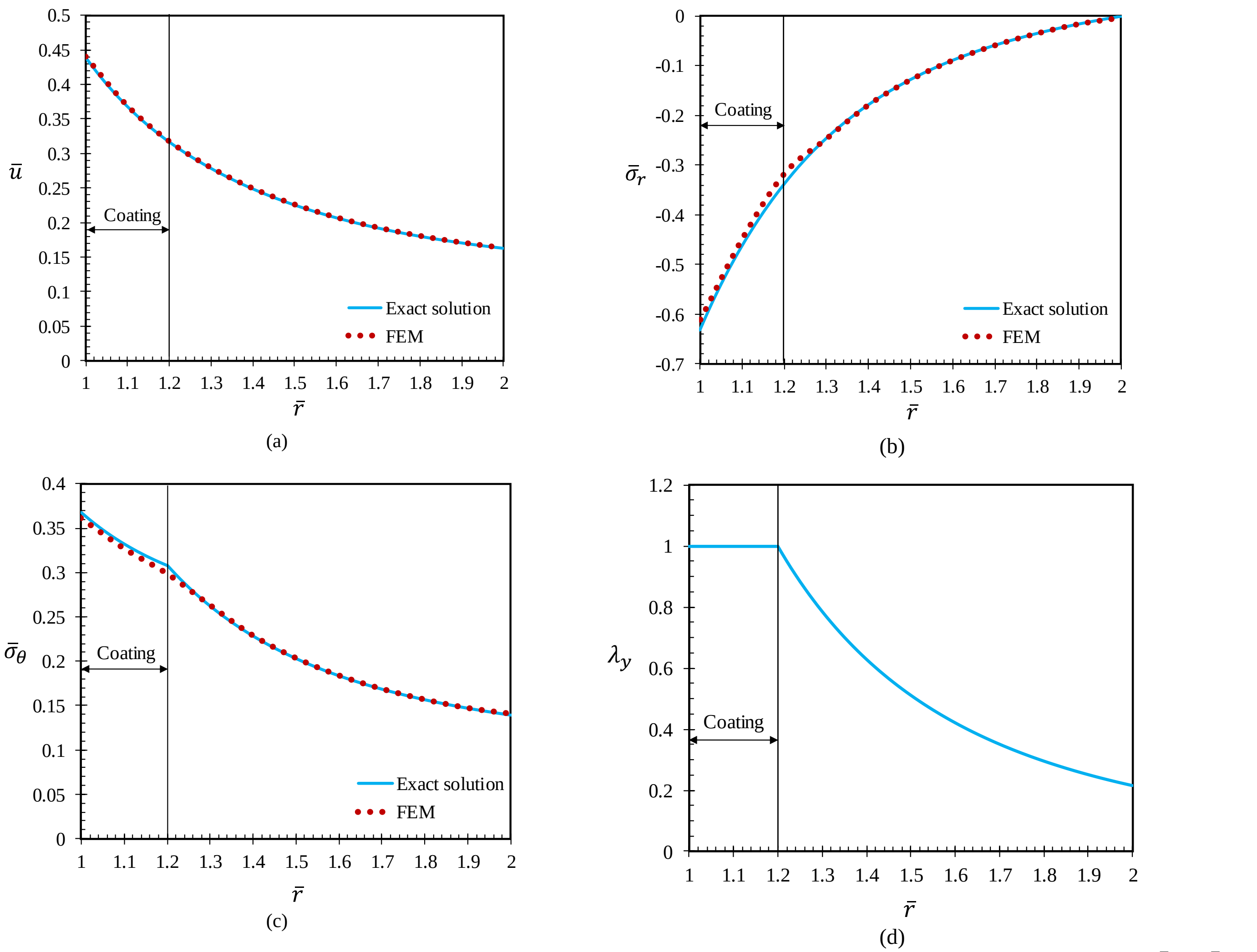

Fig. 5 Comparison of analytical results and FE solution for elastic response of internally coated spherical vessel for $n = 0.9$, $m = m_{cr} = -2.3993$ at $\bar{P}_{e1} = \bar{P}_{e2} = 0.6325$ (a) displacement (b) radial stress (c) tangential stress (d) yield variable

Considering $n = 0.9$, the effect of the parameter m on λ_y is shown in Fig. 6. The critical parameter of $m = -2.3993$ ($= m_{cr}$), $-2, -1$ and 0 is considered and the variation of the yield variable λ_y are plotted for this pressure vessel in Fig. 6. It is clear that when $m > m_{cr}$, the yielding commences at the inner surface of coating layer that is a desirable mode. By increasing the value of parameter m, the difference between radial and circumferential stresses at FG coating layer increase and lead to yielding starts later at the inner surface of homogenous structure.

Fig. 7 shows the elastic limit pressure versus the radial parameter (R_i/R_c) for different n and m values. As can be seen, the curve with $m = 0$, $n = 0$ is in agreement to homogeneous coating material. As mentioned before, for the values of $n < 0$, other modes of yielding may be occur i.e. yield commencing at the inner or outer surfaces or inside the coating layer of vessel with the same yield condition. For example, the pressure vessel with $n = -0.4$ and $m = -2$ is considered. The corresponding elastic limit pressure was obtained as $\bar{P}_e = 0.5622$ considering Tresca's yield criterion at inner surface of coating layer i.e. $\sigma_\theta{}^C(R_i) - \sigma_r{}^C(R_i) = \sigma_0(R_i)$. The consequent stresses and displacement are shown in Fig. 8. It can be seen that, the yielding also commences at the inner surface of FG coating layer.

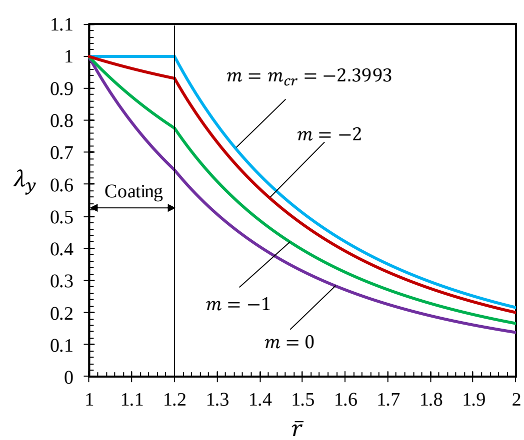

Fig. 6 Variation of yield variable in an internally coated spherical vessel for $\boldsymbol{n} = \mathbf{0.9}$ using $\boldsymbol{m}$ as a parameter

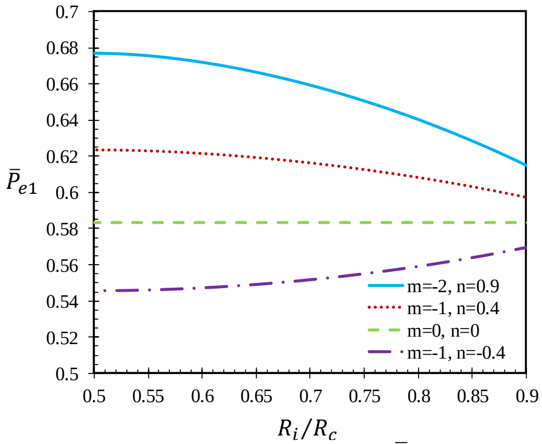

Fig. 7 Variation of elastic limit internal pressure $\bar{\boldsymbol{P}}_{\boldsymbol{e1}}$ using $\boldsymbol{n}$ and $\boldsymbol{m}$ as parameters for an internally coated spherical pressure vessel

As previously mentioned, the desired state is that the yielding starts at the inner surface of FG coating layer and the plastic region expands in the coating layer. Then the coating layer is completely deformed, plastically. Yielding commences at the inner surface of homogenous structure and the plastic deformation develops at this part. In order to establish such conditions, $n=0.9$ and $m=-1.3$ is considered. It should be noted that there are other values of graded parameters that satisfies these conditions. The corresponding elastic limit pressure was obtained as $\bar{P}_{e1}=0.6325$ considering Tresca's yield criterion at inner surface of coating layer i.e. $\sigma_\theta^{C-E}(R_i)-\sigma_r^{C-E}(R_i)=\sigma_0(R_i)$. The consequent stresses and displacement are shown in Fig. 9.

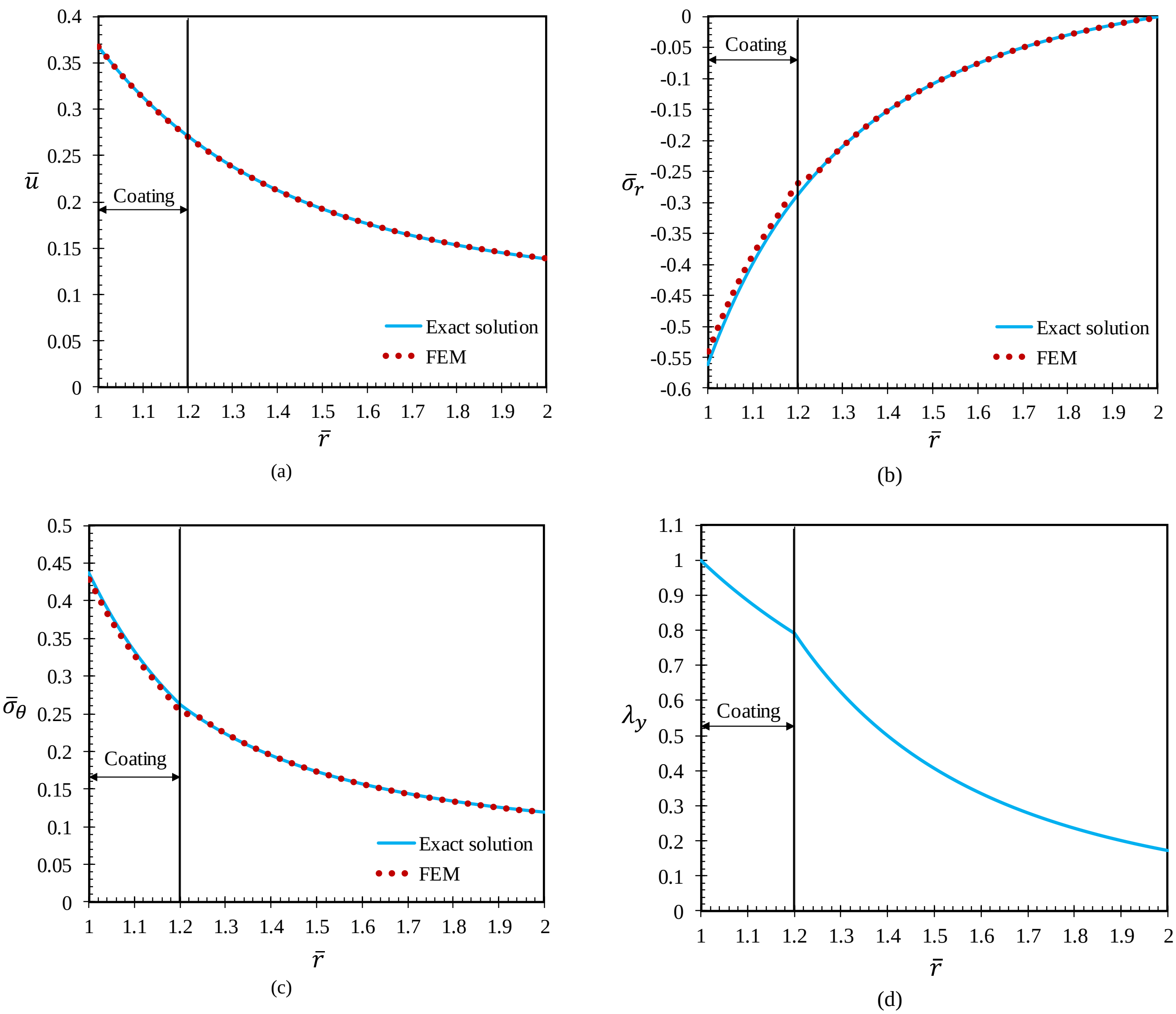

Fig. 8 Comparison of analytical results and FE solution for elastic response of internally coated spherical pressure vessel for $\boldsymbol{n}=-\boldsymbol{0.4}$, $\boldsymbol{m}=-\boldsymbol{2}$ at $\bar{\boldsymbol{P}}_{\boldsymbol{e1}}=\boldsymbol{0.5622}$ (a) displacement (b) radial stress (c) tangential stress (d) yield variable

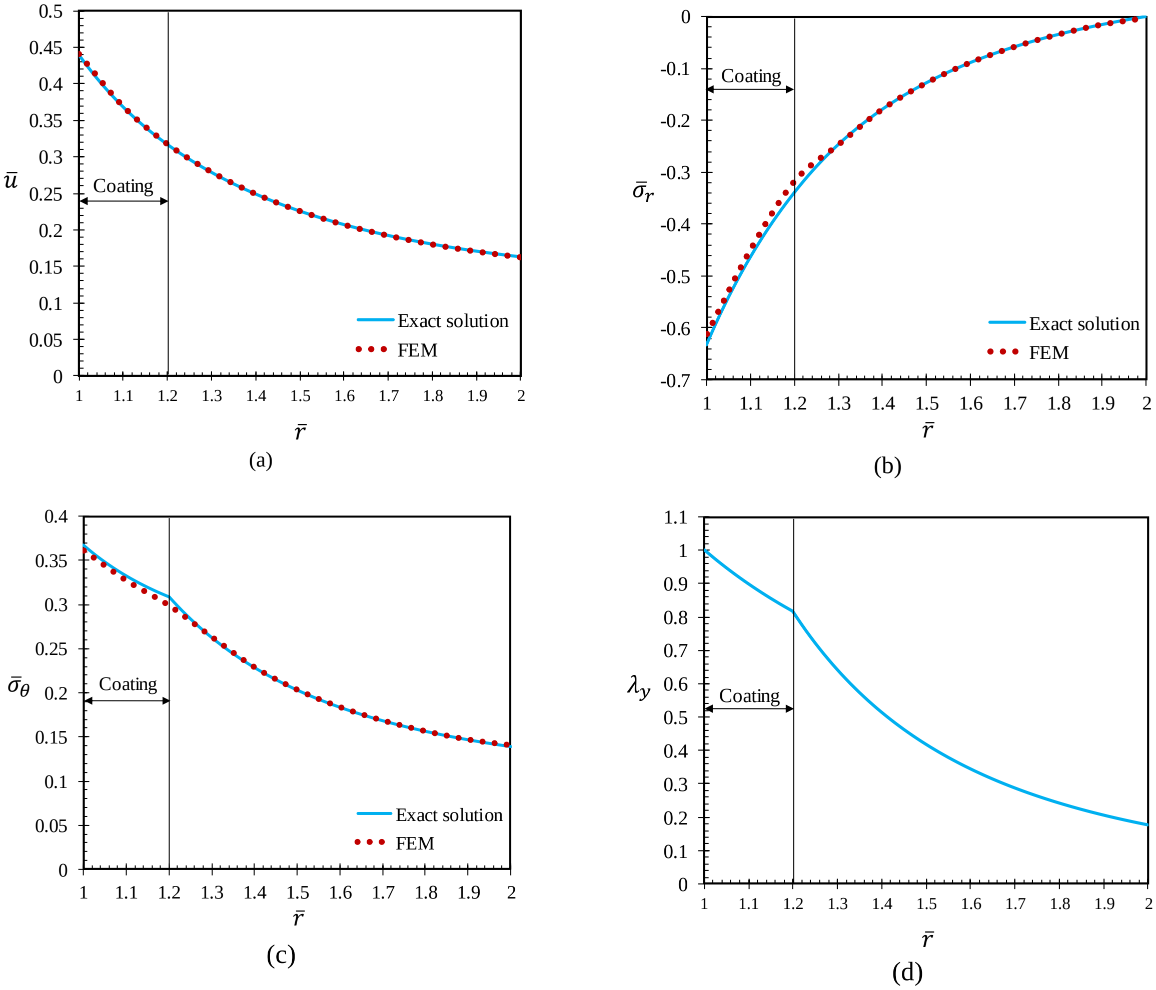

Fig. 9 Comparison of analytical results and FE solution for elastic response of internally coated spherical pressure vessel for $\boldsymbol{n} = \mathbf{0.9}$, $\boldsymbol{m} = -\mathbf{1.3}$ at $\bar{\boldsymbol{P}}_{e1} = \mathbf{0.6325}$. (a) displacement, (b) radial stress, (c) tangential stress and (d) yield variable

4.2. *Elasto-plastic*

For the internal pressure $\bar{P} > \bar{P}_{e1}$, the FG coating layer of pressure vessel is partially plastic in $R_i < r < r_{ep1}$ where r_{ep1} is the elastic - plastic border. The seven unknowns should be evaluated: C_{3F} and C_{4F} (plastic FG coating), C_{1F} and C_{2F} (elastic FG coating), C_{1H} and C_{2H} (elastic homogenous structure) and r_{ep1}. The following seven conditions are taken into account:

$$\sigma_r^{C-P}(R_i) = -P_i \tag{41}$$

$$\sigma_r^{C-P}(r_{ep1}) = \sigma_r^{C-E}(r_{ep1}) \tag{42}$$

$$\sigma_\theta^{C-P}(r_{ep1}) = \sigma_\theta^{C-E}(r_{ep1}) \tag{43}$$

$$u^{C-P}(r_{ep1}) = u^{C-E}(r_{ep1}) \tag{44}$$

$$\sigma_r^{C-E}(R_c) = \sigma_r^{H-E}(R_c) \tag{45}$$

$$u^{C-E}(R_c) = u^{H-E}(R_c) \tag{46}$$

$$\sigma_r^{H-E}(R_o) = 0 \tag{47}$$

Fig. 10 shows the evolution of the plastic region at FG coating layer of pressure vessel. Increase in $\bar{P}$ leads to expand the plastic region and the coating layer becomes fully plastic at $\bar{P} = \bar{P}_{fp1} = 0.7370$. Considering $\bar{P}$ in $\bar{P}_{e1} < \bar{P} < \bar{P}_{fp1}$, the stresses in partially plastic state could be obtained. For example, taking $\bar{P} = 0.6729$, one find $r_{ep1} = 1.0627$. Fig. 11 shows the corresponding stresses and radial displacement.

As mentioned before, when $n = 0.9$ and $m = -1.3$, the yielding commences at the inner surface of homogenous structure after fully plastic deformation in FG coating layer. The four unknowns should be evaluated: C_{3F} and C_{4F} (plastic FG coating), C_{1H} and C_{2H} (elastic homogenous structure). The following four conditions are considered:

$$\sigma_r^{C-P}(R_i) = -P_i \tag{48}$$

$$\sigma_r^{C-P}(R_c) = \sigma_r^{H-E}(R_c) \tag{49}$$

$$u^{C-P}(R_c) = u^{H-E}(R_c) \tag{50}$$

$$\sigma_r^{H-E}(R_o) = 0 \tag{51}$$

The corresponding elastic limit pressure was obtained as $\bar{P}_{e2} = 0.7370$ considering Tresca's yield criterion at the inner surface of homogenous structure i.e. $\sigma_\theta^{H-E}(R_c)-\sigma_r^{H-E}(R_c)=\sigma_c$. The consequent stresses and displacement are shown in Fig. 12

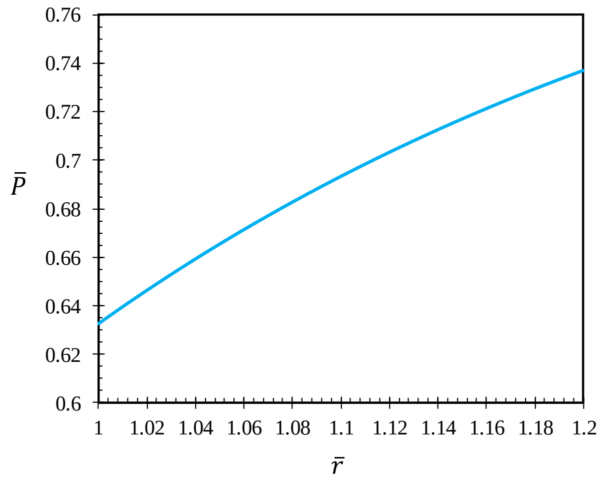

Fig. 10 Evolution of plastic region in FG coating layer of spherical pressure vessel with increasing $\bar{P}$ for $m=-1.3$ and $n=0.9$

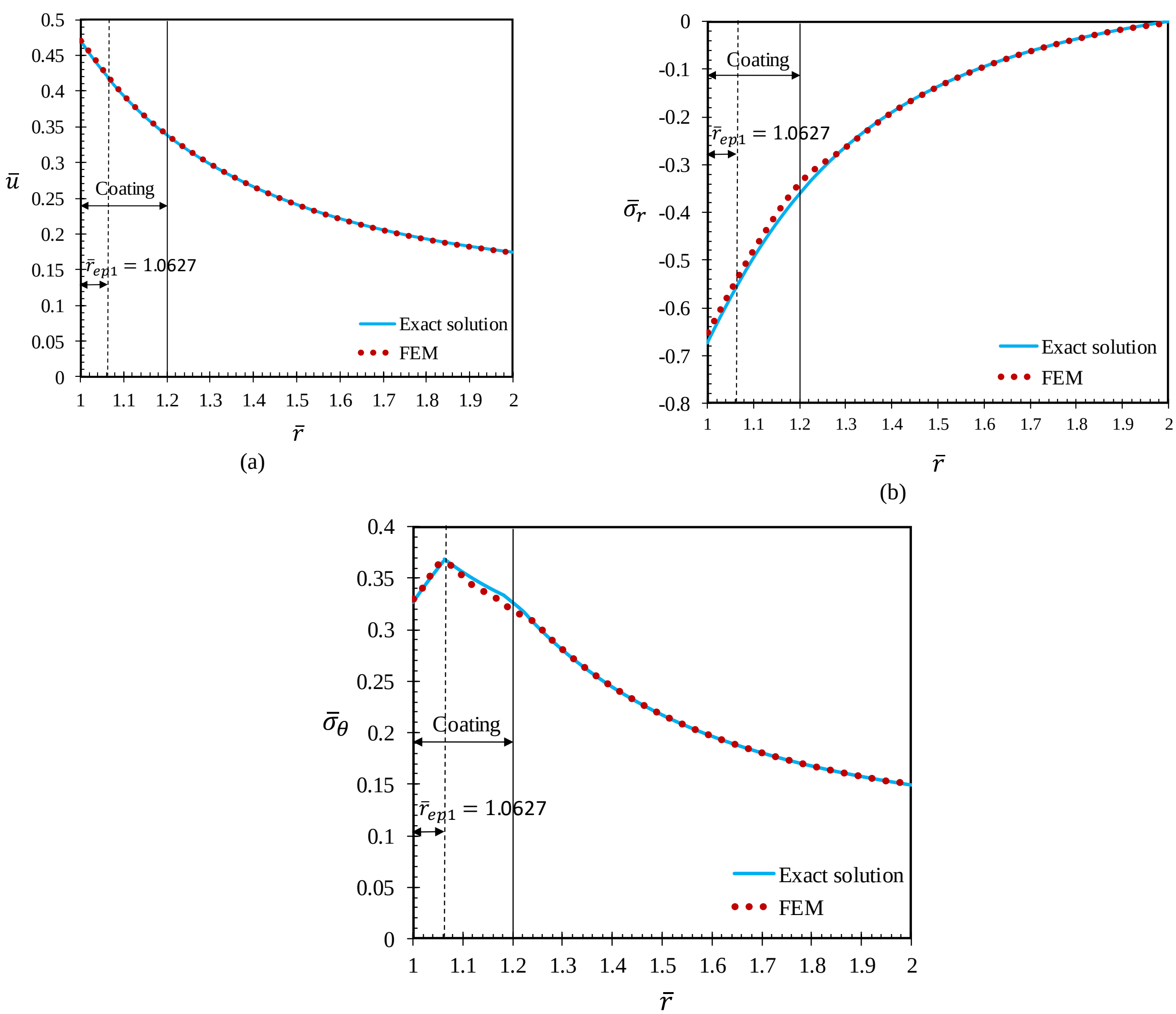

Fig. 11 Comparison of analytical results and FE solution for elastic response of internally coated spherical pressure vessel for $n=0.9$, $m=-1.3$ at $\bar{P}=0.6729$ (a) displacement (b) radial stress (c) tangential stress

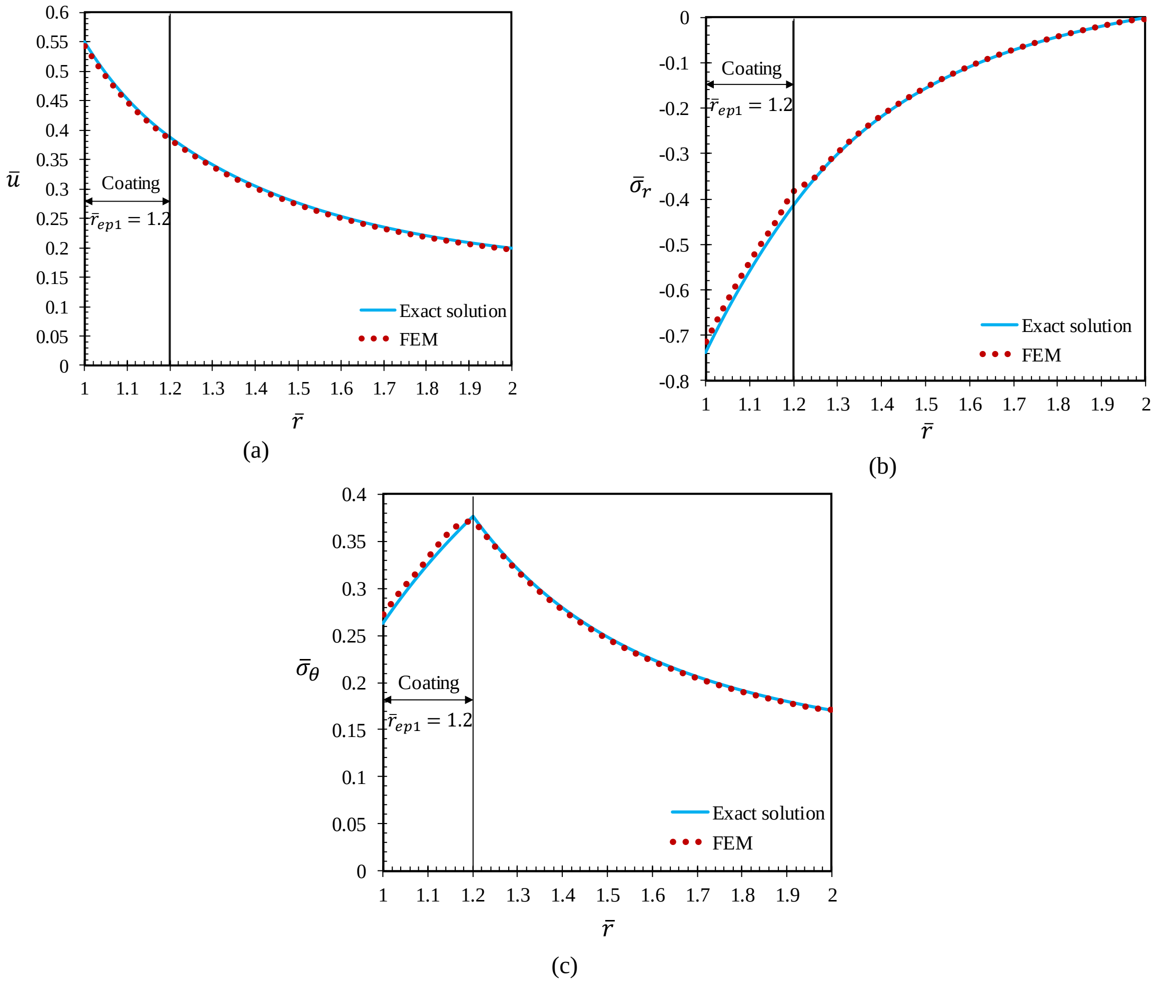

Fig. 12 Comparison of analytical results and FE solution for elastic response of internally coated spherical pressure vessel for $\boldsymbol{n = 0.9}$, and $\boldsymbol{m = -1.3}$ at $\boldsymbol{\bar{P}_{e2} = 0.7370}$ (a) displacement (b) radial stress (c) tangential stress

For the internal pressure $\bar{P} > \bar{P}_{e2}$, the homogenous structure of pressure vessel is partially plastic in $R_c \le r \le r_{ep2}$ where r_{ep2} is the plastic-elastic border. The seven unknowns should be evaluated: C_{3F} and C_{4F} (plastic FG coating), C_{1H} and C_{2H} (elastic homogenous structure), C_{3H} and C_{4H} (plastic homogenous structure) and r_{ep2}. The following seven conditions are considered:

$$\sigma_r^{C-P}(R_i) = -P_i \tag{52}$$

$$\sigma_r^{C-P}(R_c) = \sigma_r^{H-P}(R_c) \tag{53}$$

$$u^{C-P}(R_c) = u^{H-P}(R_c) \tag{54}$$

$$\sigma_\theta^{H-P}(r_{ep2}) = \sigma_\theta^{H-E}(r_{ep2}) \tag{55}$$

$$\sigma_r^{H-P}(r_{ep2}) = \sigma_r^{H-E}(r_{ep2}) \tag{56}$$

$$u^{H-P}(r_{ep2}) = u^{H-E}(r_{ep2}) \tag{57}$$

$$\sigma_r^{H-E}(R_o) = 0 \tag{58}$$

Fig. 13 shows the evolution of the plastic region at homogenous structure of pressure vessel. The increase in $\bar{P}$ leads to expand the plastic region and homogenous structure becomes fully plastic at $\bar{P} = \bar{P}_{fp2} = 1.1315$. Considering $\bar{P}$ in $\bar{P}_{e2} < \bar{P} < \bar{P}_{fp2}$, the stresses in partially plastic state could be obtained. For example, taking $\bar{P} = 0.8807$, one find $r_{ep2} = 1.3574$. Fig. 14 shows the corresponding stresses and radial displacement.

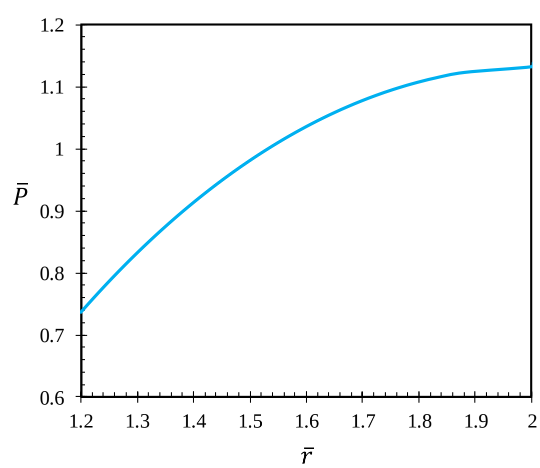

Fig. 13 Evolution of plastic region in homogenous section of spherical pressure vessel with increasing $\boldsymbol{\bar{P}}$ for $\boldsymbol{m = -1.3}$ and $\boldsymbol{n = 0.9}$

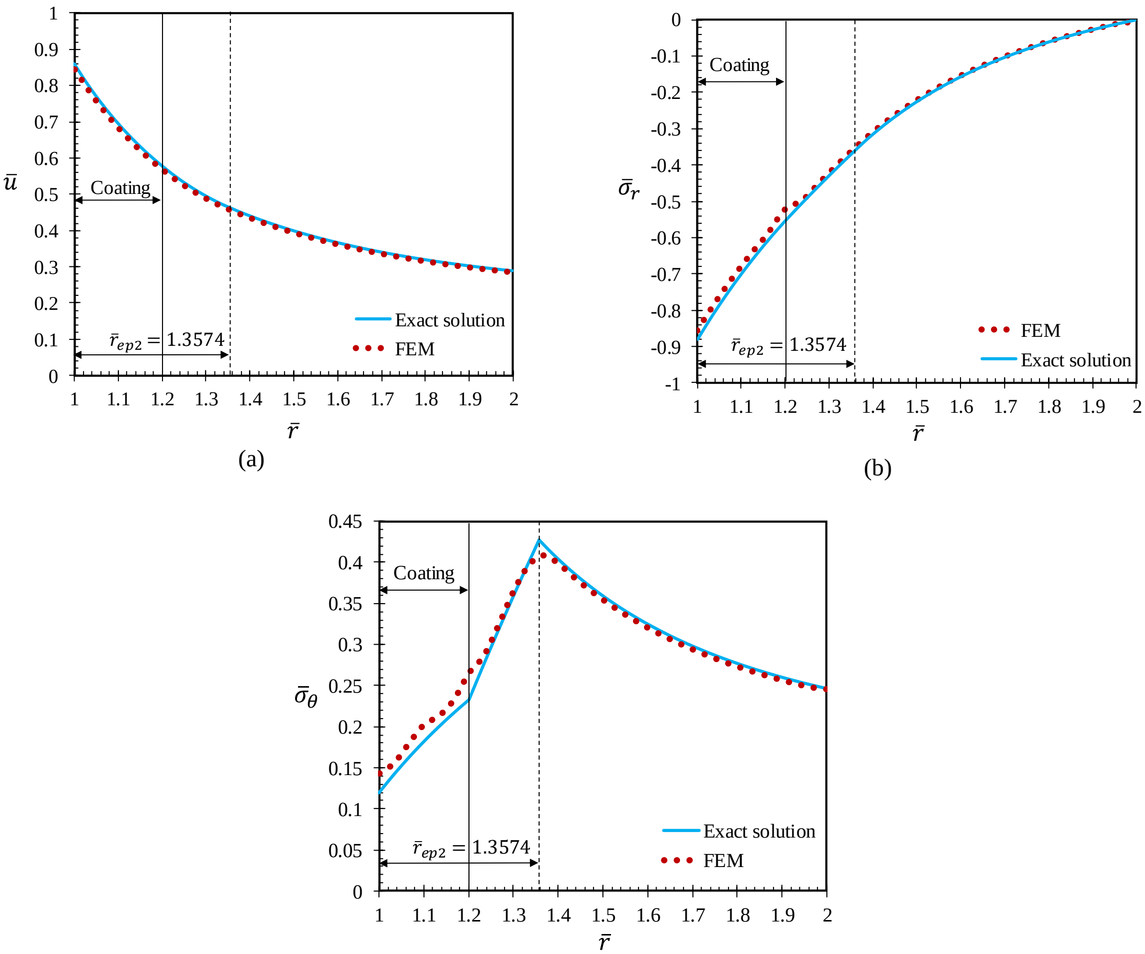

(c)

Fig. 14 Comparison of analytical results and FE solution for elastic response of internally coated spherical pressure vessel for $\boldsymbol{n = 0.9}$, and $\boldsymbol{m = -1.3}$ at $\boldsymbol{\bar{P} = 0.8807}$ (a) displacement (b) radial stress (c) tangential stress

5. Conclusion

The elasto-plastic deformation behavior of a thick spherical pressure vessel with an inner FG coating subjected to internal and external hydrostatic pressures is studied using small deformation theory and Tresca's yield criteria. The material types of vessel and coating were assumed to be homogeneous and FG, respectively. The modulus of elasticity and the uniaxial yield limit of the FG coating layer of spherical pressure vessel are considered to vary radially in nonlinear forms. These parameters for homogenous structure of pressure vessel are assumed to be constant. In this study, it is considered that the inner surface of FG coating layer is critical and plastic deformation commences at the inner surface of coating layer at the elastic limit internal pressure. Then the FG coating layer becomes fully plastic and yielding commences at the inner surface of homogenous structure. In order to satisfy this condition, the radial variation of FG parameters are established. An elastic analysis of the spherical pressure vessel was presented. Then stresses and deformation behavior of assembly was obtained using analytical expressions. Furthermore, the elasto-plastic and fully plastic response of this case are studied.

6. References

[1] S. Suresh, A. Mortensen, 1998, *Fundamentals of functionally graded materials*, The Institut of Materials,

[2] J. Aboudi, M.-J. Pindera, S. M. Arnold, Higher-order theory for functionally graded materials, *Composites Part B: Engineering*, Vol. 30, No. 8, pp. 777-832, 1999.

[3] D. Annaratone, 2007, *Pressure vessel design*, Springer,

[4] U. Schulz, M. Peters, F.-W. Bach, G. Tegeder, Graded coatings for thermal, wear and corrosion barriers, *Materials Science and Engineering: A*, Vol. 362, No. 1, pp. 61-80, 2003.

[5] H. Bufler, The arbitrarily and the periodically laminated elastic hollow sphere: exact solutions and homogenization, *Archive of Applied Mechanics*, Vol. 68, No. 9, pp. 579-588, 1998.

[6] M. Eslami, M. Babaei, R. Poultangari, Thermal and mechanical stresses in a functionally graded thick sphere, *International Journal of Pressure Vessels and Piping*, Vol. 82, No. 7, pp. 522-527, 2005.

[7] L. You, J. Zhang, X. You, Elastic analysis of internally pressurized thick-walled spherical pressure vessels of functionally graded materials, *International Journal of*

Pressure Vessels and Piping, Vol. 82, No. 5, pp. 347-354, 2005.

[8] R. Poultangari, M. Jabbari, M. Eslami, Functionally graded hollow spheres under non-axisymmetric thermo-mechanical loads, *International Journal of Pressure Vessels and Piping,* Vol. 85, No. 5, pp. 295-305, 2008.

[9] Y. Chen, X. Lin, Elastic analysis for thick cylinders and spherical pressure vessels made of functionally graded materials, *Computational Materials Science,* Vol. 44, No. 2, pp. 581-587, 2008.

[10] N. Tutuncu, B. Temel, A novel approach to stress analysis of pressurized FGM cylinders, disks and spheres, *Composite Structures,* Vol. 91, No. 3, pp. 385-390, 2009.

[11] A. Saidi, S. Atashipour, E. Jomehzadeh, Exact elasticity solutions for thick-walled fg spherical pressure vessels with linearly and exponentially varying properties, *Int J Eng Trans A,* Vol. 22, pp. 405-416, 2009.

[12] M. Sadeghian, H. E. Toussi, Axisymmetric yielding of functionally graded spherical vessel under thermo-mechanical loading, *Computational Materials Science,* Vol. 50, No. 3, pp. 975-981, 2011.

[13] E. Carrera, M. Soave, Use of functionally graded material layers in a two-layered pressure vessel, *journal of Pressure vessel Technology,* Vol. 133, No. 5, pp. 051202, 2011.

[14] A. Parvizi, R. Naghdabadi, J. Arghavani, Analysis of Al A359/SiCp functionally graded cylinder subjected to internal pressure and temperature gradient with elastic-plastic deformation, *Journal of Thermal Stresses,* Vol. 34, No. 10, pp. 1054-1070, 2011.

[15] Y. Bayat, M. Ghannad, H. Torabi, Analytical and numerical analysis for the FGM thick sphere under combined pressure and temperature loading, *Archive of Applied Mechanics,* Vol. 82, No. 2, pp. 229-242, 2012.

[16] M. Z. Nejad, M. Abedi, M. H. Lotfian, M. Ghannad, An exact solution for stresses and displacements of pressurized FGM thick-walled spherical shells with exponential-varying properties, *Journal of mechanical science and technology,* Vol. 26, No. 12, pp. 4081, 2012.

[17] M. S. Boroujerdy, M. Eslami, Thermal buckling of piezo-FGM shallow spherical shells, *Meccanica,* Vol. 48, No. 4, pp. 887-899, 2013.

[18] M. Saadatfar, M. Aghaie-Khafri, Hygrothermomagnetoelectroelastic analysis of a functionally graded magnetoelectroelastic hollow sphere resting on an elastic foundation, *Smart Materials and Structures,* Vol. 23, No. 3, pp. 035004, 2014.

[19] A. Parvizi, S. Alikarami, M. Asgari, Exact solution for thermoelastoplastic behavior of thick-walled functionally graded sphere under combined pressure and temperature gradient loading, *Journal of Thermal Stresses,* Vol. 39, No. 9, pp. 1152-1170, 2016.

[20] S. Alikarami, A. Parvizi, Elasto-plastic analysis and finite element simulation of thick-walled functionally graded cylinder subjected to combined pressure and thermal loading, *Science and Engineering of Composite Materials*.

[21] T. Akis, Elastoplastic analysis of functionally graded spherical pressure vessels, *Computational Materials Science,* Vol. 46, No. 2, pp. 545-554, 2009.

[22] S. A. Atashipour, R. Sburlati, S. R. Atashipour, Elastic analysis of thick-walled pressurized spherical vessels coated with functionally graded materials, *Meccanica,* Vol. 49, No. 12, pp. 2965-2978, 2014.

[23] A. Loghman, H. Parsa, Exact solution for magneto-thermo-elastic behaviour of double-walled cylinder made of an inner FGM and an outer homogeneous layer, *International Journal of Mechanical Sciences,* Vol. 88, pp. 93-99, 2014.

[24] Z. Wang, Q. Zhang, L. Xia, J. Wu, P. Liu, Thermomechanical analysis of pressure vessels with functionally graded material coating, *Journal of Pressure Vessel Technology,* Vol. 138, No. 1, pp. 011205, 2016.

[25] A. Afshin, M. Zamani Nejad, K. Dastani, Transient thermoelastic analysis of FGM rotating thick cylindrical pressure vessels under arbitrary boundary and initial conditions, *Journal of Computational Applied Mechanics,* Vol. 48, No. 1, pp. 15-26, 2017.

[26] M. Gharibi, M. Zamani Nejad, A. Hadi, Elastic analysis of functionally graded rotating thick cylindrical pressure vessels with exponentially-varying properties using power series method of Frobenius, *Journal of Computational Applied Mechanics,* Vol. 48, No. 1, pp. 89-98, 2017.

[27] R. Ghajar, M. Shokrieh, A. R. Shajari, Transient thermo-visco-elastic response of a functionally graded non-axisymmetric cylinder, *Journal of Computational Applied Mechanics,* Vol. 46, No. 2, pp. 191-204, 2015.

[28] S. Timoshenko, 1934, *Theory of Elasticity*, McGraw-Hill,

[29] A. Mendelson, 1968, *Plasticity: theory and application*, Macmillan,

[30] A. Nayebi, S. A. Sadrabadi, FGM elastoplastic analysis under thermomechanical loading, *International Journal of Pressure Vessels and Piping,* Vol. 111, pp. 12-20, 2013.